Click Here for Full Article

Dimethylsulphide, clouds, and phytoplankton: Insights from a simple plankton ecosystem feedback model

Roger Cropp,[1] John Norbury,[2] and Roger Braddock[1]

Received 9 August 2006; revised 13 November 2006; accepted 5 April 2007; published 14 June 2007.

[1] The hypothesis that marine plankton ecosystems may effectively regulate climate by the production of dimethylsulphide (DMS) has attracted substantial research effort over recent years. This hypothesis suggests that DMS produced by marine ecosystems can affect cloud properties and hence the averaged irradiance experienced by the phytoplankton that produce DMS's precursor dimethylsulphoniopropionate (DMSP). This paper describes the use of a simple model to examine the effects of such a biogenic feedback on the ecosystem that initiates it. We compare the responses to perturbation of a simple marine nitrogen-phytoplankton-zooplankton (*NPZ*) ecosystem model with and without biogenic feedback. Our analysis of this heuristic model reveals that the addition of the feedback can increase the model's resilience to perturbation and hence stabilize the model ecosystem. This result suggests the hypothesis that DMS may play a role in stabilizing marine plankton ecosystem dynamics through its effect on the atmosphere.

Citation: Cropp, R., J. Norbury, and R. Braddock (2007), Dimethylsulphide, clouds, and phytoplankton: Insights from a simple plankton ecosystem feedback model, *Global Biogeochem. Cycles*, *21*, GB2024, doi:10.1029/2006GB002812.

1. Introduction

[2] The prospect of human-induced climate change has stimulated research into several biological processes that might affect climate. One such process that has attracted a substantial research effort is the so-called CLAW hypothesis [*Charlson et al.*, 1987]. This hypothesis suggests that marine plankton ecosystems may effectively regulate climate by a feedback associated with the production of dimethylsulphide (DMS). *Charlson et al.* [1987] observed that some of the DMS produced by marine ecosystems is transferred from the ocean to the atmosphere where it is the major source of cloud condensing nuclei (CCN) over the remote oceans. The aerosols resulting from biogenic DMS emissions can have a direct effect on the solar radiative forcing experienced by the Earth through scattering, absorption and reflection and can also lead to increased cloud formation; the CLAW hypothesis proposes that these mechanisms could regulate climate. *Charlson et al.* [1987] argued that an increase in global temperature would lead to increased biogenic DMS emissions from the ocean and result in an increase in scattering, cloud cover and cloud albedo that would increase the proportion of the incoming solar radiation reflected back into space (thus changing the global albedo), and thereby cooling the planet.

[3] DMS is an ecosystem product. Many species of marine phytoplankton synthesize dimethylsulphoniopropionate (DMSP), the precursor to DMS. However, most DMSP that is converted to DMS is done so by ecosystem processes that occur outside the phytoplankton cell [*Simó*, 2001]. In addition to the climatic role postulated for DMS by the CLAW hypothesis, DMSP is a compatible solute that can protect cells from the osmotic effects of seawater and the effects of freezing, may deter predation by zooplankton, may act as an antioxidant, and has also been proposed to assist in the long-range dispersal of marine phytoplankton [*Hamilton and Lenton*, 1998; *Kiene et al.*, 2000; *Sunda et al.*, 2002; *Wolfe et al.*, 1997].

[4] The objective of this paper is to examine the implications of the climate regulation process proposed by *Charlson et al.* [1987] for the dynamics of the ecosystems that produce it. To do this we develop a simple plankton model that incorporates the DMS feedback mechanism and compare its dynamics to the same ecosystem model without the feedback. The plankton model is composed of nutrient (*N*), phytoplankton (*P*) and zooplankton (*Z*), and is one of a class of *NPZ* models that have proved powerful heuristic tools in biological oceanography [*Franks*, 2002]. The feedback processes quantified by *Charlson et al.* [1987] (a changed light environment arising from a modified albedo due to DMS production, where the changed light environment then influences the phytoplankton growth rate) were incorporated into the *NPZ* model to build a biogenic feedback model that was not intrinsically constrained to any specific oceanic environment. The structure of this model is shown in Figure 1. Our whole-of-system modeling approach is similar to that of *Lawrence* [1993], who used a similar model to assess the impact of the feedback on climate. Our approach and intention is substantially different: we close the feedback cycle on the ecosystem, and

[1]Centre for Environmental Systems Research, Faculty of Environmental Sciences, Griffith University, Nathan, Queensland, Australia.
[2]Mathematical Institute, University of Oxford, Oxford, UK.

Copyright 2007 by the American Geophysical Union.
0886-6236/07/2006GB002812$12.00

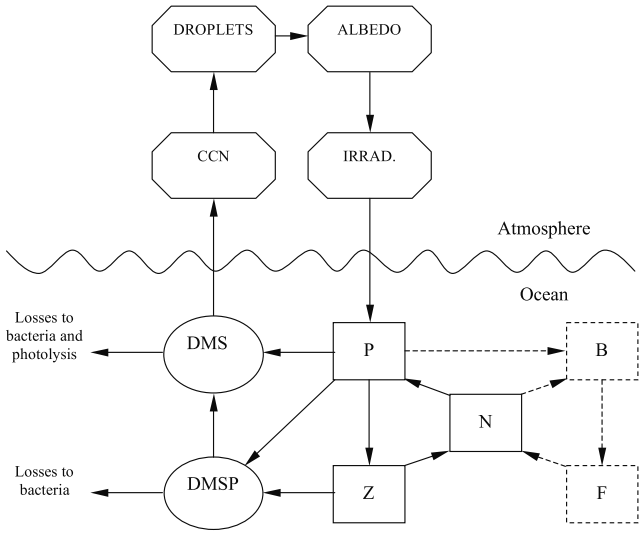

Figure 1. Schematic diagram of the *NPZ-DMS* feedback model. Dotted lines indicate the components of the original GMSK model that have been omitted for this analysis.

examine the implications of the feedback for the ecosystems that generate it.

[5] Comparisons between simulations of the *NPZ* model with and without feedback were undertaken to elucidate the influence of the feedbacks for the ecosystem. The simulations revealed that the presence of the feedback generally enhanced the stability of the ecosystem by making it more resilient to perturbation. Resilience is a form of stability that may be analytically evaluated for many simple ecosystem models. The resilience of model ecosystems is defined as the negative of the dominant eigenvalue of the linearized system about the steady state [*DeAngelis*, 1980], and is inversely related to the time the model ecosystem will take to return to its equilibrium state after a perturbation.

[6] A sensitivity analysis of the model with instantaneous feedback (the reason we examine instantaneous feedback is discussed) indicated that such feedback always stabilized the system, that is no parameter values or combination of parameter values used in the sensitivity analysis caused the system to become less stable than the equivalent system without the feedback. We note that the feedback system is more sensitive to the magnitude and direction of zooplankton perturbations than to phytoplankton perturbations. We also note the sensitive dependence of the feedback effect on time lags in the feedback process, and the influence of the biometric rate parameters on these effects. These parameters are also important determinants of the resilience of the ecosystem model.

2. Ecosystem Model

[7] We first describe the basic *NPZ-DMS* model without feedback, summarized in equations (1)–(5), and the methods used in this analysis. We then develop the feedback model (equation (34) and equations (35)–(37)).

2.1. *NPZ-DMS* Model

[8] A simple model of a planktonic ecosystem that produces DMS is used as the starting point for this analysis. The model is a simplification of the GMSK model proposed by *Gabric et al.* [1993], in which a *DMS-DMSP* model was coupled to the plankton ecosystem model of *Moloney et al.* [1986]. This model is shown in Figure 1, where it comprises all the model components in the ocean. The ecosystem model has been simplified to a nutrient-phytoplankton-zooplankton (*NPZ*) model, a valuable tool in biological oceanography [*Franks*, 2002], for this analysis and coupled to the DMS equations of *Gabric et al.* [1993]. A schematic of the resulting simple *NPZ-DMS* model comprises the model components shown as solid lines in the ocean in Figure 1.

[9] The *NPZ-DMS* model is defined by the following equations:

$$\frac{dN}{dt} = k_5 Z + k_3 k_4 PZ - k_1 \left(\frac{N}{N+k_2}\right) P\,, \tag{1}$$

$$\frac{dP}{dt} = k_1 \left(\frac{N}{N+k_2}\right) P - k_3 PZ\,, \tag{2}$$

$$\frac{dZ}{dt} = k_3 (1-k_4) PZ - k_5 Z\,, \tag{3}$$

$$\frac{dDMSP}{dt} = m_1 \gamma P + m_2 \gamma Z - m_3 DMSP - m_4 DMSP\,, \tag{4}$$

$$\frac{dDMS}{dt} = \gamma m_5 P + m_3 DMSP - m_6 DMS - m_7 DMS. \tag{5}$$

[10] Equations (1)–(3) represent the ecosystem component of the model. These equations are written in a currency of nitrogen (where N, P and Z represent the concentrations of dissolved inorganic nutrient, phytoplankton and zooplankton respectively in units of atomic nitrogen). These equations conserve mass so that $N + P + Z = N_T$ always, where N_T is the total nutrient in the system. Equations (4) and (5) represent the DMS production generated by the ecosystem and are written in a currency of sulphur (where *DMSP* and *DMS* represent the concentrations of dimethylsulphoniopropionate and dimethylsulphide respectively in units of atomic sulphur) and these equations do not conserve mass. The k and m parameters represent the attributes of biota in the ecosystem model and the rates of chemical reactions and physical processes in the DMS model. The parameter γ in equations (4) and (5) represents the sulphur:nitrogen ratio of marine plankton. The parameter set used by *Gabric et al.* [1999], derived from measured values reported in the literature, was selected as a starting point for this analysis (Table 1, G99). The equations derived by

Table 1. Parameters and Values for the *NPZ-DMS* Model

Parameter	Process	Unit	Value	
			G99[a]	GA[b]
k_1	maximum rate of N uptake by P	d^{-1}	0.27	0.9918
k_2	half-saturation constant for P uptake of N	mgN m^{-3}	12.6	19.1230
k_3	Z grazing rate (per individual) on P	$m^3 mgN^{-1} d^{-1}$	0.02	0.0256
k_4	proportion of N uptake excreted by Z	-	0.3	0.0287
k_5	Z specific mortality rate	d^{-1}	0.050	0.3720
m_1	rate of release of *DMSP* by P	d^{-1}	0.01	0.0076
m_2	rate of *DMSP* excretion rate by Z	d^{-1}	0.01	0.3050
m_3	*DMSP* – *DMS* conversion rate	d^{-1}	0.5	0.9226
m_4	rate of *DMSP* consumption by bacteria	d^{-1}	0.53	0.1201
m_5	rate of release of *DMS* by P	d^{-1}	0.0085	0.0045
m_6	rate of *DMS* consumption by bacteria	d^{-1}	0.29	0.2664
m_7	maximum *DMS* photo-oxidation rate	d^{-1}	1.3	0.5752
γ	phytoplankton *S(DMSP):N* ratio	mg S/mg N	0.3	0.3580
N_T	total nutrient as dissolved inorganic nitrogen	mgN m^{-3}	50	3.0761

[a]G99 represents *Gabric et al.* [1999].
[b]GA represents derived by GA for model validation in this paper.

Gabric et al. [1993] were used as the basis for developing a feedback process to incorporate in the *NPZ* model to create the biofeedback model. This is described in section 2.3.

2.2. *NPZ* Model Resilience

[11] The nitrogen-based components of the *NPZ-DMS* model may be isolated to form an ecosystem (*NPZ*) model. This model has four critical (equilibrium) points defined by $\frac{dN}{dt} = \frac{dP}{dt} = \frac{dZ}{dt} = 0$ of which one is ecologically infeasible and two are unstable and not relevant to this analysis (see *Cropp and Norbury* [2007] for details). The fourth point is an asymptotically stable node located at

$$P^* = \frac{k_5}{k_3(1-k_4)}, \tag{6}$$

$$Z^* = \frac{k_1}{k_3}\left(\frac{N^*}{N^*+k_2}\right), \tag{7}$$

$$N^* = \frac{1}{2}\left[-\left(k_2 + P^* + \frac{k_1}{k_3} - N_T\right) \pm \sqrt{\left(k_2 + P^* + \frac{k_1}{k_3} - N_T\right)^2 - 4k_2(P^* - N_T)}\right]. \tag{8}$$

[12] The eigenvalues of the linearized *NPZ* model about this point are

$$\lambda = -\frac{k_1 P^*}{2}\left[\frac{k_2}{(N^*+k_2)^2}\right] \cdot \left\{1 \pm \sqrt{1 - (N^*+k_2)\left[1 + \frac{(N^*+k_2)^2}{k_1 k_2 P^*}\right]\left(\frac{4k_4 N^*}{k_2 P^*}\right)}\right\}. \tag{9}$$

[13] For the parameter values used in this study (and for most reasonable values) this point is an asymptotically stable spiral node, indicating that when the model is perturbed from this steady state it will oscillate in "boom-and-bust" cycles of decreasing amplitude until it regains equilibrium. The amplitude and rate of decay of these cycles is determined by the magnitude of the real part of the eigenvalue of this point, the basis of *DeAngelis'* [1980] resilience measure,

$$\text{Res} = \frac{k_1}{2}\left(\frac{k_2}{(N^*+k_2)^2}\right)\left(\frac{k_5}{k_3(1-k_4)}\right). \tag{10}$$

[14] This resilience metric is inversely proportional to the time required for the model to return to equilibrium after a perturbation and we will use this metric to describe the stability of the model.

[15] High resilience means that a system will rapidly return to its steady state after a perturbation. *Johnson* [1990] studied isolated Arctic lake ecosystems and proposed the hypothesis that ecosystems adapt to acquire attributes that endow the system with high resilience. *Cropp and Gabric* [2002] simulated the adaptation of a simple plankton ecosystem model under thermodynamic constraints and modified Johnson's hypothesis to propose that ecosystems adapted to states of maximum resilience within genetic and environmental constraints. *Laws* [2003] reported that the concept of maximum resiliency was a useful heuristic for fitting ecosystem models to observed plankton data in many regions of the global oceans.

2.3. Feedback Model

[16] The feedback model is based on the simplified GMSK model and comprises of the *NPZ* model described above coupled to a model of the sulphur and atmospheric processes. The feedback model is also shown in Figure 1, and comprises all the model components drawn with solid lines in both the ocean and the atmosphere.

[17] A *DMS* submodel may be extracted from the sulphur-based components of the *NPZ-DMS* model (equations (4)–(5))

for analysis. A steady state of the *DMS* submodel may be obtained where the aqueous *DMS* concentration is defined in terms of *P, Z* and some parameters,

$$DMS^* = \gamma\left(\frac{P(m_1m_3 + m_5m_3 + m_5m_4) + m_2m_3Z}{(m_3 + m_4)(m_6 + m_7)}\right). \quad (11)$$

[18] This steady state is always an asymptotically stable node, and for measured parameter values the eigenvalues of this point are large and negative, indicating that the steady state is a strong attractor and the *DMS* model is highly resilient. This means that the system will return to its steady state very rapidly after any perturbation, and that the steady state values are a therefore a good description of the system. Analytic expressions describing $P(t)$ and $Z(t)$ are not derivable, but it is clear that the *DMS* model is essentially slaved to the *NPZ* model, and the state of the ecosystem model will determine the state of the *DMS* model. These properties of the *NPZ-DMS* model allow the effects of the system's feedback on its own environment to be included in a simple ecosystem biofeedback model. The derivation of this model is now described.

2.4. DMS Sea-Air Transfer

[19] The flux of DMS from the ocean to the atmosphere (DMS_{flux}) may be modeled as a linear function of the aqueous concentration of DMS (DMS_{aq}) and the DMS piston velocity (k_{tr}) [*Liss and Merlivat*, 1986],

$$DMS_{flux} = k_{tr}DMS_{aq}\,. \quad (12)$$

[20] Although this flux occurs only at the ocean surface, when applied in a zero-dimensional (i.e., depth-averaged over the mixed layer) model as in this analysis, the loss of DMS_{aq} is also averaged over the depth of the mixed layer (*MLD*),

$$DMS_{flux} = \left(\frac{k_{tr}}{MLD}\right)DMS_{aq}\,. \quad (13)$$

[21] The DMS piston velocity parameterizes the rate at which DMS is transferred from the ocean to the atmosphere, and the empirically derived estimate of *Nightingale et al.* [2000] was used in this analysis:

$$k_{tr} = 0.005\left(5.88u_{10}^2 + 1.49u_{10}\right)Sc^{-1/2}\,, \quad (14)$$

where k_{tr} (day^{-1}) is for a notional 48-m-deep mixed layer, u_{10} is the 10-m wind speed (m s^{-1}) and *Sc* is the dimensionless Schmidt number. The Schmidt number is temperature-dependent, and the experimentally derived relationship of *Saltzman et al.* [1993] was used,

$$Sc = 2764 - 147.12\,SST + 3.726\,SST^2 - 0.038\,SST^3\,, \quad (15)$$

where *SST* is the sea surface temperature (°C). The sea surface temperature has little influence on the piston velocity, which is mostly controlled by the wind speed. A global average wind speed of 8.2 m s^{-1} (derived from two years of SeaWinds 12 hourly measurements) and a global average sea surface temperature of 16.7°C (derived from 15 years of Advanced Very High Resolution Radiometer (AVHRR) data) were used for this analysis, giving a representative DMS piston velocity of k_{tr} = 2.88 m d^{-1}. This is consistent with the estimates of *Simó and Dachs* [2002] who used a nonlinear correction to zonal monthly climatological wind speeds and obtained global estimates of piston velocity between 1 and 4 m d^{-1}.

[22] A relationship between *P*, *Z* and *DMS* flux from the ocean to the atmosphere can be derived by substituting equation (11) into equation (12),

$$\begin{aligned} DMS_{flux} &= k_{tr}\gamma\left[\frac{(m_1m_3 + m_3m_5 + m_4m_5)}{(m_3 + m_4)(m_6 + m_7)}P + \frac{m_2m_3}{(m_3 + m_4)(m_6 + m_7)}Z\right] \\ &= k_6P + k_7Z, \end{aligned} \quad (16)$$

where $k_6 = \frac{\gamma k_{tr}(m_1m_3 + m_3m_5 + m_4m_5)}{(m_3 + m_4)(m_6 + m_7)}$, and $k_7 = \frac{\gamma k_{tr}m_2m_3}{(m_3 + m_4)(m_6 + m_7)}$ where k_6 and k_7 have units of mgS m mgN^{-1} d^{-1} and DMS_{flux} has units of mgS m^{-2} d^{-1}.

2.5. DMS Flux and Cloud Condensation Nuclei

[23] *Pandis et al.* [1994] estimated a long-term average cloud condensation nuclei (CCN)−DMS flux relationship over the remote ocean from the steady state of a model of the principal gas-, aerosol- and aqueous-phase processes in the marine atmospheric boundary layer. They predicted that when DMS emission flux is smaller than 1.3 μmoles m^{-2} d^{-1} the CCN concentration is essentially constant at 20 particles cm^{-3}. In a second DMS flux regime, extending between 1.3 and 2.3 μmoles m^{-2} d^{-1} only a few particles become CCN each day. A third region corresponds to DMS emission fluxes larger than 2.3 μmoles m^{-2} d^{-1}. The CCN concentration in this regime is a linear function of the DMS flux,

$$CCN = 22.7DMS_{flux} - 15.0, \quad (17)$$

where *DMS* emission flux is in μmoles m^{-2} d^{-1} and *CCN* is in particles cm^{-3}. *Simó and Dachs* [2002] estimated a conservative global mean annual flux of DMS from the ocean to the atmosphere of 6.8 μmoles m^{-2} d^{-1} (σ = 2.49 μmoles m^{-2} d^{-1}) suggesting that equation (17) is appropriate for a globally representative model. Converting this relationship to represent *DMS* in mg S m^{-2} d^{-1} using 1 μmol S m^{-2} d^{-1} = 0.032 mgS m^{-2} d^{-1} gives approximately

$$CCN = 710DMS_{flux} - 15. \quad (18)$$

[24] When applied using *Simó and Dachs'* [2002] global mean DMS flux estimate equation (18) produces a CCN estimate of 140 particles cm^{-3}, comparable to CCN observations of 50−250 particles cm^{-3} reported for the Northeast Atlantic Ocean by *Hegg* [1994]. Substituting equation (16) into equation (18) then gives

$$\begin{aligned} CCN &= 710(k_6P + k_7Z) - 15 \\ &= k_8(k_6P + k_7Z) - k_9. \end{aligned} \quad (19)$$

where k_8 = 710 and k_9 = 15.

2.6. Cloud Condensation Nuclei and Cloud Droplets

[25] Several authors have derived relationships between *CCN* and cloud droplet number concentration (N_C) (see *Gondwe* [2004] for a summary). The empirically measured relationships reported in the literature take several forms, although they all describe similar (hyperbolic-like) relationships. In keeping with our heuristic approach, we have used the simple nonlinear relationship between cloud droplet number (N_C) and the number of *CCN* measured by *Saxena and Menon* [1999] over the southeastern United States,

$$\begin{aligned} N_C &= 183\ln(CCN) - 334 \\ &= k_{10}\ln(CCN) - k_{11} \end{aligned}, \tag{20}$$

where $k_{10} = 183$ and $k_{11} = 334$. This relationship is similar (differing only slightly in the coefficients) to the relationship between *CCN* and the subcloud aerosol number concentration measured over the North Atlantic Ocean by *Gultepe and Isaac* [1996]. It also produces estimates of N_C similar to the theoretical derivation of *Chuang and Penner* [1995] (when applied with the associated relationship between *CCN* and sulphate aerosol mass concentration given by *Saxena and Menon* [1999]) suggesting equation (20) is a robust parameterization. Substituting equation (19) into equation (20) gives an estimate of the number of cloud droplets that will result from *DMS* ventilated into the atmosphere from the ecosystem,

$$N_c = k_{10}\ln[k_8(k_6P + k_7Z) - k_9] - k_{11}. \tag{21}$$

2.7. Cloud Droplets, Albedo, and Irradiance

[26] Relationships between changes in cloud droplet number and changes in cloud top albedo (α), assuming constant atmospheric liquid content, have been provided by several authors [*Han et al.*, 1998]. These are all similar linear relationships, varying only in the slope, and the most recent, given by *Schwartz and Slingo* [1996], and valid for albedos between 0.28 and 0.72, is used here:

$$\begin{aligned} \Delta\alpha &\approx 0.075\left(\frac{\Delta N}{N_0}\right) \\ &\approx 0.075\left(\frac{N_C - N_0}{N_0}\right) \end{aligned}, \tag{22}$$

where N_0 is the reference cloud droplet number density and ΔN is the change in cloud droplet concentration from the reference. The change in cloud top albedo due to change in the flux of DMS from the ocean to the atmosphere can then be approximated by substituting equation (21) into equation (22),

$$\begin{aligned} \Delta\alpha &= 0.075\left\{\frac{k_{10}\ln[k_8(k_6P + k_7Z) - k_9] - k_{11} - N_0}{N_0}\right\} \\ &= k_{12}\left\{\frac{k_{10}\ln[k_8(k_6P + k_7Z) - k_9] - k_{11} - N_0}{N_0}\right\} \end{aligned}, \tag{23}$$

where $k_{12} = 0.075$.

[27] If it is assumed that the reference number of droplets (N_0) is equated with the steady state of the ecosystem (i.e., the reference number of droplets includes a contribution from the ecosystem at steady state), then N_0 can be described in terms of the steady state values of the *NPZ* model,

$$N_0^* = k_{10}\ln[k_8(k_6P^* + k_7Z^*) - k_9] - k_{11}, \tag{24}$$

where P^* and Z^* are defined by equations (6) and (7) respectively. The change in cloud top albedo attributable to a change in DMS production by the ecosystem is then given by

$$\Delta\alpha = \frac{k_{12}}{N_0^*}\left\{k_{10}\ln[k_8(k_6P + k_7Z) - k_9] - k_{11} - N_0^*\right\}. \tag{25}$$

2.8. Irradiance and Photosynthesis

[28] The depth of mixing in the upper ocean influences the average irradiance experienced by phytoplankton. This also varies latitudinally, seasonally and daily with values of 30 m typical of equatorial regions, and 100 m typical of high latitudes. The average mixed layer irradiance at any latitude may be approximated by

$$I_A = \frac{I_\theta}{MLD}\int_0^{MLD} e^{-k_L z}\,dz = \frac{I_\theta}{MLD}\left(\frac{1 - e^{-k_L MLD}}{k_L}\right), \tag{26}$$

where I_A is the average irradiance over the mixed layer; $I_\theta = I_E\cos(\theta)$ is the incident surface irradiance at latitude θ; I_E is the incident surface irradiance at the equator; *MLD* is the depth of the mixed layer; z is depth in the water column in meters; and k_L is the seawater light extinction coefficient (typically 0.04 m^{-1} for ocean water).

[29] *Zonneveld* [1998] derived a photosynthesis-irradiance (*PI*) curve of the general form

$$P_{photo} = \frac{aI_P}{bI_P^2 + I_P + c}, \tag{27}$$

where P_{photo} denotes photosynthesis, I_P denotes irradiance measured as the average number of photons per area per time, a represents the maximum rate quantum yield per photosynthetic unit, b represents the ratio of the cell absorption cross section to the specific recovery rate of damaged d-protein, and c represents the excitation requirements of the cell. Zonneveld observed that other researchers had derived relationships of the same general form from different premises.

[30] Phytoplankton acclimate to the average light intensity in which they grow [*Zonneveld*, 1998], and it is therefore reasonable to assume that phytoplankton throughout the

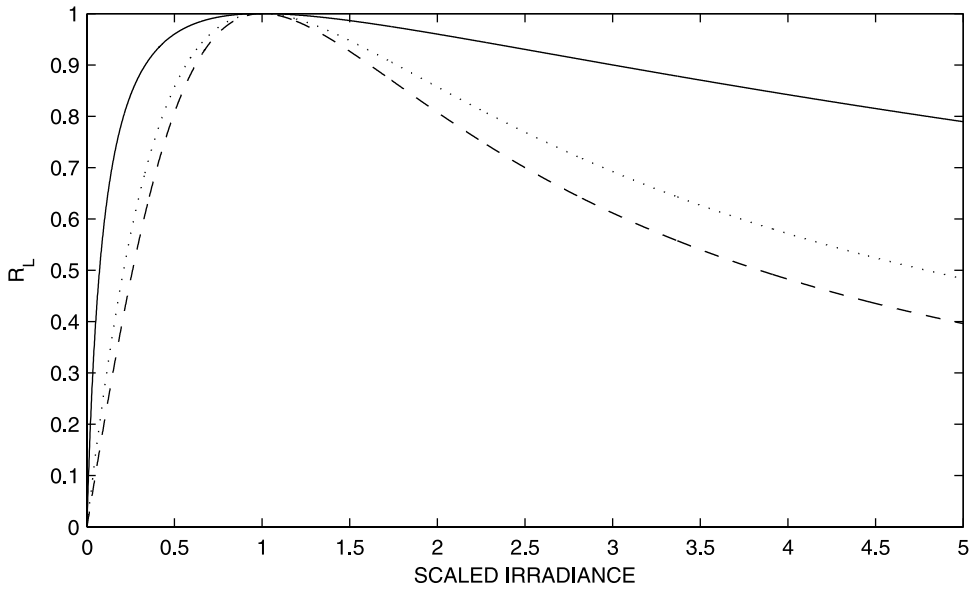

Figure 2. Photosynthesis-irradiance curve described by equation (30). Solid line is $b = 0.10$, dotted line is $b = 1$, and dashed line is $b = 10$.

global oceans are adapted to their local irradiance. The average irradiance experienced by endemic phytoplankton at any latitude on the globe (I_A) may then be scaled by their saturating irradiance (I_S, at which phytoplankton photosynthesis is a maximum), and the effect of variations in irradiance on phytoplankton growth at any latitude may then be approximated by

$$P_{photo} = \frac{aI}{bI^2 + I + c}, \tag{28}$$

where $I = \frac{I_A}{I_S}$. The maximum value of equation (28) occurs when

$$I = \sqrt{\frac{c}{b}}, \tag{29}$$

and the maximum value of P_{photo} is now by definition achieved when $I = 1$, which from equation (29) stipulates that $c = b$. The *PI* relationship may be applied to a particular phytoplankton species by scaling it to be a function between 0 and 1 that operates on the maximum phytoplankton growth rate (k_1) of the phytoplankton species. This condition specifies that P_{photo} $(I = 1) = 1$, and therefore equation (28) stipulates that $a = 1 + 2b$. The photosynthesis-irradiance relationship may then be written as a general nondimensional operator on the maximum phytoplankton growth rate,

$$R = \frac{(1 + 2b)I}{bI^2 + I + b}, \tag{30}$$

where b is now a photo-inhibition parameter that controls the shape of the *PI* curve (Figure 2) and is likely to be species-dependent. Note that R is relatively insensitive to b once $b > 1$. As b tends toward infinity R tends to $\frac{2I}{I^2+1}$, so when $b = \infty$, $R = 0.385$ at $I = 5$, not appreciably different to its value when for example $b = 10$, when $R = 0.396$.

[31] The R curves in Figure 2 represent a dimensionless operator on the maximum phytoplankton growth rate, and equation (2) in the ecosystem model becomes

$$\frac{dP}{dt} = k_1 R\left(\frac{N}{N + k_2}\right)P - k_3 PZ, \tag{31}$$

and the appropriate modification is also made to equation (1),

$$\frac{dN}{dt} k_5 Z + k_3 k_4 PZ - k_1 R\left(\frac{N}{N + k_2}\right)P. \tag{32}$$

[32] The usual condition when the climate is unperturbed (by anthropogenic or biogenic activities) has $I = 1$ (as we have previously assumed $I = \frac{I_A}{I_S}$ in equation (28)). Any perturbations to this steady state due to ecosystem feedbacks such as described by equation (23) will affect the irradiance experienced by the phytoplankton, and can be modeled by replacing the irradiance in equation (30) with the term $1 - \Delta\alpha$, representing the change in irradiance due to changes in albedo,

$$R = \frac{(1 + 2b)(1 - \Delta\alpha)}{b(1 - \Delta\alpha)^2 + (1 - \Delta\alpha) + b}. \tag{33}$$

[33] This feedback effect may be written in terms of P and Z by substituting for $\Delta\alpha$ from equation (25) giving an

expression describing the effect on a marine planktonic ecosystem of its production of DMS,

$$R = \frac{(1+2k_{13})\left(1-\frac{k_{12}}{N_0^*}\{k_{10}\ln[k_8(k_6P+k_7Z)-k_9]-k_{11}-N_0^*\}\right)}{k_{13}\left(1-\frac{k_{12}}{N_0^*}\{k_{10}\ln[k_8(k_6P+k_7Z)-k_9]-k_{11}-N_0^*\}\right)^2+\left(1-\frac{k_{12}}{N_0^*}\{k_{10}\ln[k_8(k_6P+k_7Z)-k_9]-k_{11}-N_0^*\}\right)}, \quad (34)$$

where k_{13} has been substituted for b.

2.9. Feedback Model

[34] A global biogeochemical feedback model incorporating the effects of DMS produced by marine ecosystems on climate and irradiance, and therefore their own environment, can now be written by incorporating equation (34) into the *NPZ* model (equations (1)–(3)),

$$\frac{dN}{dt} = k_5Z + k_3k_4PZ - Rk_1\left(\frac{N}{N+k_2}\right)P, \quad (35)$$

$$\frac{dP}{dt} = Rk_1\left(\frac{N}{N+k_2}\right)P - k_3PZ, \quad (36)$$

$$\frac{dZ}{dt} = k_3(1-k_4)PZ - k_5Z, \quad (37)$$

where R is given by equation (34). The values of the additional parameters (k_6–k_{13}) used for the feedback model simulations are listed in Table 2. The nature of the scaling described in the model formulation ensures that the steady states of the simple and feedback models are identical (i.e., at steady state $R = 1$).

2.10. Time-Lagged Feedback Model

[35] The time-lagged feedback model was developed by including a time lag (τ) in the feedback term,

$$R = \frac{(1+2k_{13})\left(1-\frac{k_{12}}{N_0^*}\{k_{10}\ln[k_8(k_6P(t-\tau)+k_7Z(t-\tau))-k_9]-k_{11}-N_0^*\}\right)}{k_{13}\left(1-\frac{k_{12}}{N_0^*}\{k_{10}\ln[k_8(k_6P(t-\tau)+k_7Z(t-\tau))-k_9]-k_{11}-N_0^*\}\right)^2+\left(1-\frac{k_{12}}{N_0^*}\{k_{10}\ln[k_8(k_6P(t-\tau)+k_7Z\ (t-\tau))-k_9]-k_{11}-N_0^*\}\right)+k_{13}} \quad (38)$$

so that phytoplankton growing at time (t) experience light conditions determined by *DMS* emissions generated by the P and Z populations at some earlier time ($t - \tau$).

3. Methods

3.1. *NPZ-DMS* Model Validation

[36] Often the only model validation available for ecosystem models is to test whether a model can reproduce observed data [*Franks*, 2002], and the *NPZ-DMS* model (equations (1)–(5)) used in this analysis was evaluated against this criteria in a study region in the Southern Ocean off the eastern Antarctic coast (60°S–65°S, 125°E–140°E). The model was formulated as a seasonally forced, depth-averaged model for the validation, where the state variables were averaged over the depth of the surface ocean mixed layer and the model was forced with climatologies of environmental data. The forcings comprised ocean mixed layer depth (*MLD*), sea surface temperature (*SST*), photosynthetically active radiation (*PAR*) and sea surface wind speed (*WIN*), and were sourced from the World Oceanographic Atlas, and from the Pathfinder, SeaWiFS and SeaWinds satellite sensors respectively. Time series of the forcings are shown in Figure 3.

[37] Annual climatologies of ocean surface chlorophyll and DMS concentrations for the study region were developed from SeaWiFS satellite data and the *Kettle et al.* [1999] database respectively. Model P values in mg N m^{-3} were converted to mg Chl a m^{-3} assuming a Redfield C:N ratio of 5.7 (by weight) and a typical carbon:chlorophyll ratio of 50 [*Walsh et al.*, 2001] for the comparison. A genetic algorithm, an efficient nonlinear optimization technique that does not require any derivative information [*Holland*, 1975; *Mitchell*, 1997], was used to fit the model to observed data by minimizing the squared error between the model predictions and the observed data. A parameter set was derived for the forced *NPZ* model so that the P population reproduced the surface ocean chlorophyll concentrations climatology. The *NPZ-DMS* model was then fitted to the DMS climatology.

[38] Seasonal forcing is implemented in the depth-averaged form of the *NPZ-DMS* model by replacing k_1 in equations (1) and (2) with k_1', where

$$k_1' = R_LR_Tk_1, \quad (39)$$

where R_T is the temperature limitation of the phytoplankton growth rate and R_L is the light limitation of the phytoplankton growth rate. The light limitation factor R_L

Table 2. Additional Parameters Derived for the Biofeedback Model

Parameter	Process	Unit	Value
k_6	*P-DMS* flux parameter	mgS m mgN^{-1} d^{-1}	0.0128
k_7	*Z-DMS* flux parameter	mgS m mgN^{-1} d^{-1}	0.0035
k_8	*CCN-DMS* flux ratio	m^{2}d mgS^{-1}	710
k_9	*CCN* background level	-	15
k_{10}	N_C-*CCN* ratio	-	183
k_{11}	N_C-*CCN* regression constant	-	334
k_{12}	$\Delta\alpha$-N_C ratio	-	0.075
k_{13}	phytoplankton *PI* curve parameter	-	$0 - \infty$
N_0	$\Delta\alpha - N_C$ reference droplet number (N_0)	-	-

is used to explicitly represent the measured seasonal forcing of light in driving chlorophyll and hence DMS dynamics for the model validation (where it must reproduce seasonal variations in chlorophyll and DMS). In contrast the light factor R (equation (34)) represents the feedback light limitation due to changes in albedo, and is free of seasonal effects in an unforced model.

[39] Laboratory studies of phytoplankton have revealed a dependence of phytoplankton growth rates on temperature [*Eppley*, 1972; *Goldman and Carter*, 1974]. The temperature dependence of phytoplankton growth used in the model validation was estimated by *Eppley* [1972] to be

$$R_T = e^{0.063(T - T_{max})}, \tag{40}$$

where T is the ambient temperature (°C) and T_{max} is the maximum annual temperature. R_T was forced with the climatology of SST (Figure 3a) for the validation.

[40] As noted previously, the average irradiance in the ocean mixed layer (I_A) can be approximated by equation (26). For the purposes of the model validation, a form of light limitation on the phytoplankton growth rate proposed by *Walsh et al.* [2001] was used,

$$R_L = \frac{I_A}{I_S} e^{\left(1 \frac{I_A}{I_S}\right)}, \tag{41}$$

where I_S the phytoplankton saturating irradiance (assumed to be 35 W m^{-2} for this analysis [*Walsh et al.*, 2001, and references therein]). R_L was forced with the climatologies of MLD and PAR (Figures 3b and 3c) for the validation.

[41] The *DMS* model (equations (4) and (5)) was modified for the validation exercise by including a term parameterizing the transfer of DMS from the ocean to the atmosphere identical to that used in the feedback model (equations (12)–(15)). However, the *DMS* sea-air transfer velocity (k_{tr}) was forced by the climatologies of SST and WIN (Figures 3a and 3d) for the validation exercise.

3.2. Perturbation Analysis

[42] The eigenvalues of the *NPZ* model are easily derived and informative; however, the eigenvalues of the biofeedback model are not. The effect of including the feedback on the model dynamics was therefore evaluated by numerically calculating the time required for each model to return to steady state after a perturbation. The return time of a system provides a useful measure of its resilience as defined by *DeAngelis* [1980], to which it is inversely proportional.

[43] The models are reactive in the sense of *Neubert and Caswell* [1997] in that they respond to almost all perturbations by initially amplifying the magnitude of the perturba-

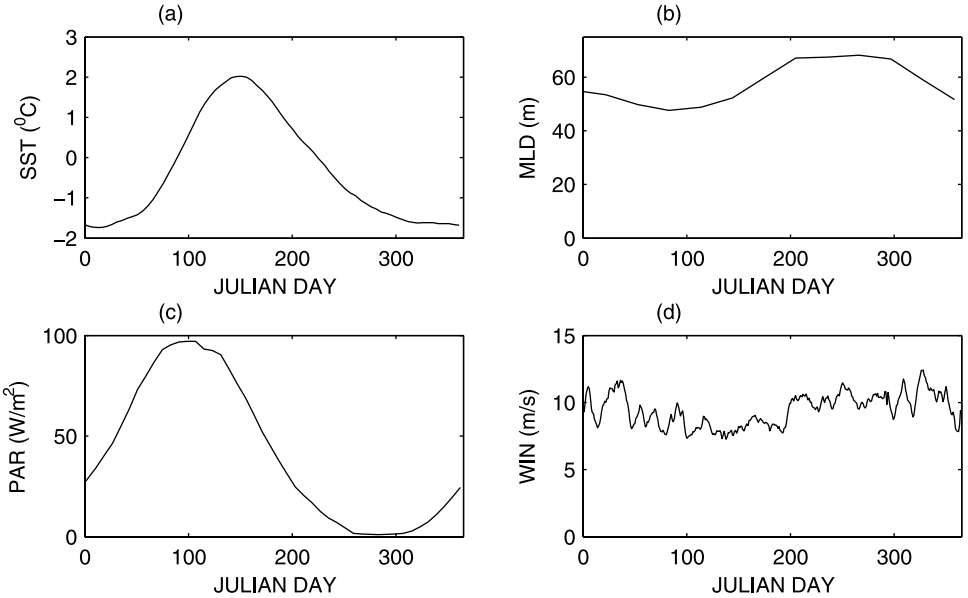

Figure 3. Forcing data for depth-averaged *NPZ-DMS* model validations: (a) sea surface temperature (SST), (b) mixed layer depth (MLD), (c) photosynthetically active radiation (PAR), and (d) sea surface wind speed (WIN) for the Southern Ocean region 60°S–65°S, 125°E–140°E.

tion, after which the perturbation exponentially decays as the model returns to its steady state. A simple metric measuring the closeness of the model trajectory to steady state was not therefore possible, and the time required for the whole of the model's trajectory to be confined within a circle of 0.05% of the area of the model's state-space was therefore used. The accuracy of this metric is determined by the period of oscillation of the system and is approximately controlled by the imaginary part of the linearized nonfeedback system's eigenvalue given by

$$Err \approx \pm\frac{2\pi}{\mathrm{Im}(\lambda)} = \pm 4\pi^{-2}\sqrt{\left[k_1\left(\frac{k_2}{(N^*+k_2)^2}\right)P^*\right]^2 - 4P^*\left[k_3k_4Z^* - k_1\left(\frac{N^*}{N^*+k_2}\right)\right]\left[k_3 - k_1\left(\frac{k_2}{(N^*+k_2)^2}\right)P^*\right]}. \quad (42)$$

[44] Return time surfaces were calculated for each of the models to demonstrate the effect of the inclusion of the feedback process on the model resilience. These surfaces were generated by perturbing each model 400 times using combinations of perturbations of −90 to +100% (in steps of 10%) of the steady state values of P and Z (equations (6) and (7), respectively). The models were integrated forward in time using the perturbed steady state values as initial conditions for the integration. Return time surfaces were generated for each model and normalized by the largest return time of the nonfeedback model. A difference surface describing the effect of the feedback was also calculated. Although the return time surfaces appear quite smooth, the accuracy constraints of the metric used to build them meant that the difference surface was not smooth. The difference surface was therefore smoothed for display; however, the smoothing did not change the fundamental characteristics of the surface.

3.3. Sensitivity Analysis

[45] A sensitivity analysis of the biofeedback model was undertaken to ascertain the most important parameters and processes in the model and to evaluate its behavior. The New Morris Method, an efficient second-order screening method [*Campolongo and Braddock*, 1999; *Cropp and Braddock*, 2002] was used for the sensitivity analysis. The sensitivity analysis measured the difference in return time surfaces of the models. This analysis quantified the sensitivity of the feedback effect to the model parameters, and is an important part of the analysis because, as was evident in the development of the feedback model, the empirical relationships used have poorly known parameter values. Two sensitivity metrics were calculated: the sum of the differences between the return times of the models for each perturbation,

$$F = \sum_{i=1}^{20}\sum_{j=1}^{20}\left(R_{N:1,j} - R_{F:i,j}\right), \quad (43)$$

where $R_{N:\,i,\,j}$ is the return time for the *NPZ* model from perturbation (i, j) and $R_{F:\,i,\,j}$ is the equivalent return time of the feedback model, and the normalized equivalent,

$$F_N = \sum_{i=1}^{20}\sum_{j=1}^{20}\left(\frac{R_{N:1,j} - R_{F:i,j}}{R_{N:1,j}}\right). \quad (44)$$

[46] The sensitivity analysis was implemented to examine the influence of the 22 parameters of the feedback model (k_1–k_5, k_8–k_{13}, m_1–m_7 and γ; see Tables 1 and 2) and was implemented using parameter ranges of ±25% of the values listed in Tables 1 (G99) and 2. The analysis made 48,400 comparisons of return time surfaces and required 3.87×10^7 model evaluations.

3.4. Time Lag Analysis

[47] The inclusion of the feedback time lag analysis recognizes that a delay between a phytoplankton bloom and increased DMS concentration in the water has been observed [*Turner et al.*, 2004, 1996] and that time lags between the transfer of DMS to the atmosphere and modification of irradiance are likely to be significant. As none of the relationships used to build the feedback model are reported with associated timescales, the feedback model by default includes the assumption that the atmospheric processes of the feedback occur instantaneously. Clearly this assumption is untenable, and hence we have also examined the effect of time lags in the feedback process on our simulation results.

[48] The effect of time lags in the feedback processes was examined by modifying the feedback model to include a time lag into the feedback R that operates on the P growth term (see feedback model description above). However, there is little conclusive evidence indicating the magnitude of the time lags involved in these processes [*Ayers and Gillett*, 2000]. In situ correlations of ocean-atmosphere DMS flux, atmospheric DMS concentration and condensation nuclei [*Andreae et al.*, 1995] have suggested that some pathways may be as short as six hours [*Lin and Chameides*, 1993]. In the absence of definitive evidence to the contrary, a reasonable first approximation is to commence the time lags at zero and increase them until interesting model behavior appears exhausted.

[49] A numerical analysis of the difference between the return time surfaces of the *NPZ* model and the time-lagged feedback model was conducted for time lags between 0 and 15 days. The perturbation metric selected ensured that the model was integrated for approximately 1500 days, about a hundred times longer than the largest time lag, ensuring the discontinuities related to the initial conditions did not affect the return times. Return time surfaces were calculated for

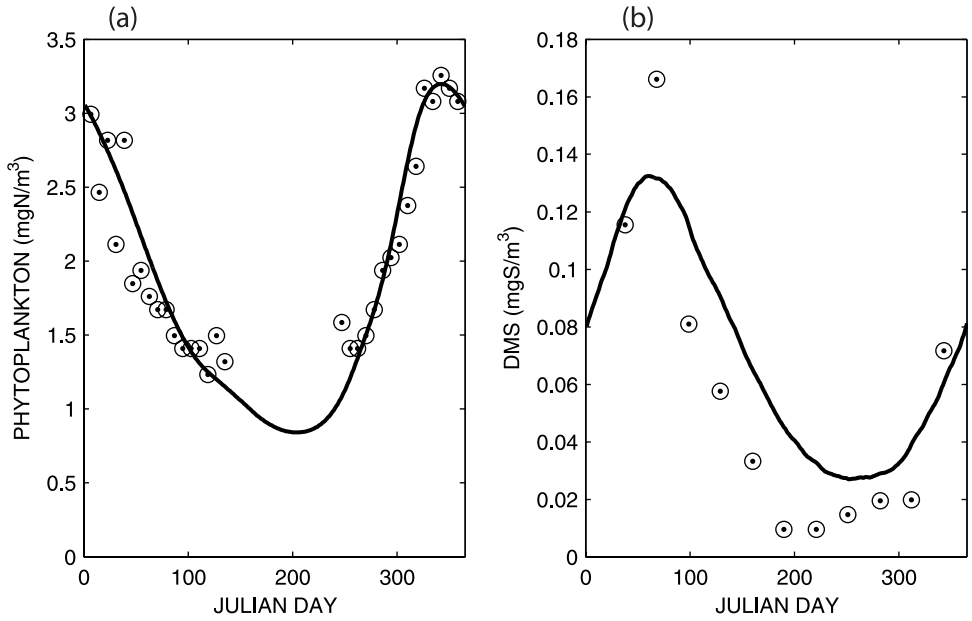

Figure 4. Best fits derived for depth-averaged *NPZ-DMS* model validations: (a) model *P* (line) and SeaWiFS chlorophyll data (dots) and (b) model *DMS* (line) and *Kettle et al.* [1999] DMS data (dots). Data are for the same Southern Ocean region as Figure 3.

60 time lags between 0.25 and 15 days in increments of 0.25 days. These return time surfaces were each subtracted from the return time surface of the *NPZ* model and the resulting difference surface was summed to give a scalar metric of the feedback effect for each time lag. This metric was scaled by the sum of the return time surface of the equivalent *NPZ* model to provide a proportional measure of the feedback effect. This enabled comparison of the feedback effects between different parameterizations as they have very different magnitude return time surfaces.

[50] The ecosystem model contains three rate parameters: the phytoplankton maximum growth rate (k_1), the rate of zooplankton grazing on phytoplankton (k_3) and the rate of zooplankton mortality (k_5). Previous sensitivity analysis of the major determinants of DMS flux to the atmosphere [*Cropp et al.*, 2004] have identified the importance of k_1 and k_3. These results are confirmed by the importance of these parameters to the feedback effect examined in this research (see below), which also identified k_5 as an important determinant of the magnitude of the feedback effect. The time

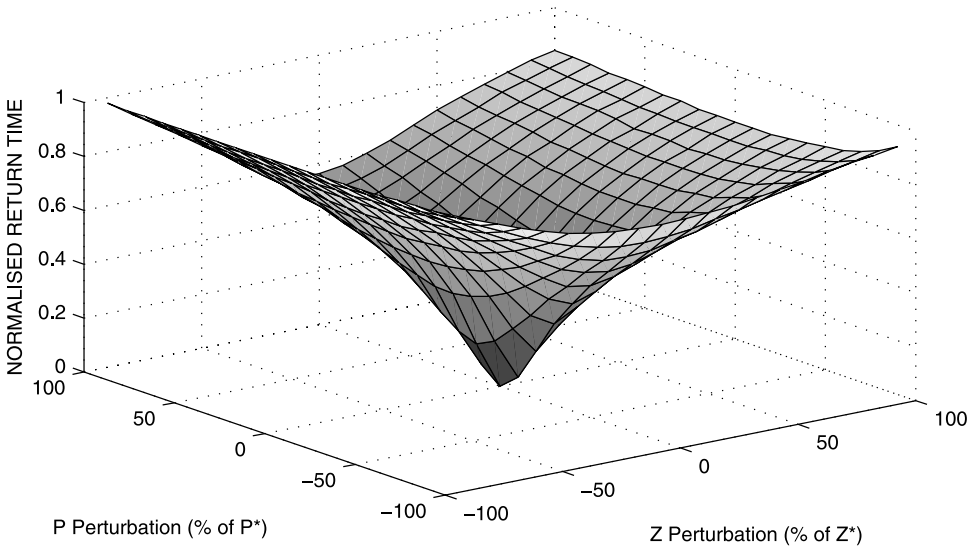

Figure 5. Normalized return time surface for the *NPZ-DMS* model without feedback showing the times the system takes to return to its equilibrium state after perturbation.

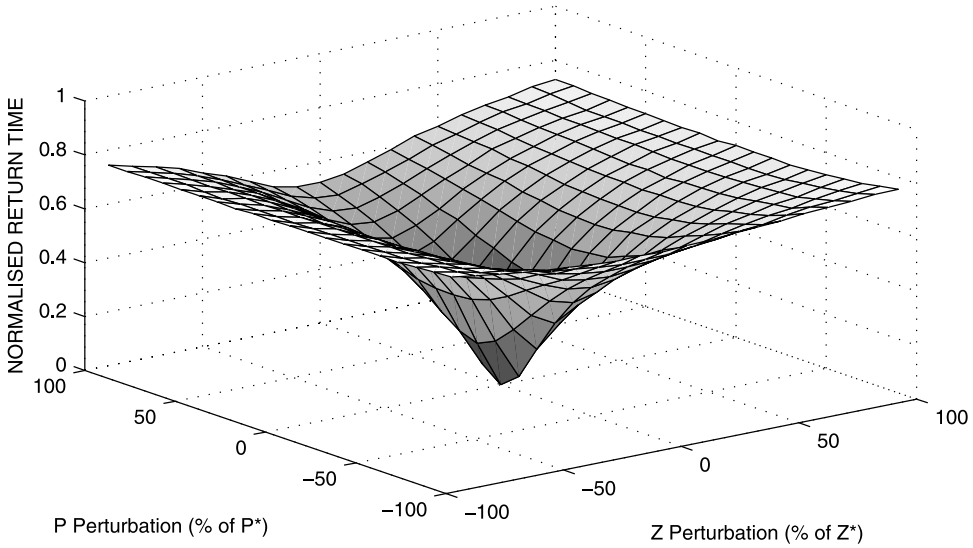

Figure 6. Normalized return time surface for the *NPZ-DMS* model with feedback showing the times the system takes to return to its equilibrium state after perturbation.

lag analysis was therefore conducted for the basic parameter set and also for parameter sets with doubled k_1, doubled k_3 or doubled k_5.

4. Results

4.1. *NPZ-DMS* Model Validation

[51] The *P* concentration predicted by the depth-averaged *NPZ* model for the best fit parameter set derived by the genetic algorithm is shown in Figure 4a with the SeaWiFS chlorophyll data. Similarly, the best fit to the interpolated DMS data derived by *Kettle et al.* [1999] is shown in Figure 4b. (The environmental forcings used in the simulation are shown in Figure 3.) The parameter values used to generate the predictions in Figure 4 are listed in Table 1 (GA). The model produces a prediction that matches the observed data well, suggesting that the *NPZ* model is a valid representation of the generic plankton seasonal dynamics in the region of the Southern Ocean off the east Antarctic coast, and similarly that the *DMS* model is a valid representation of the seasonal DMS dynamics in this region.

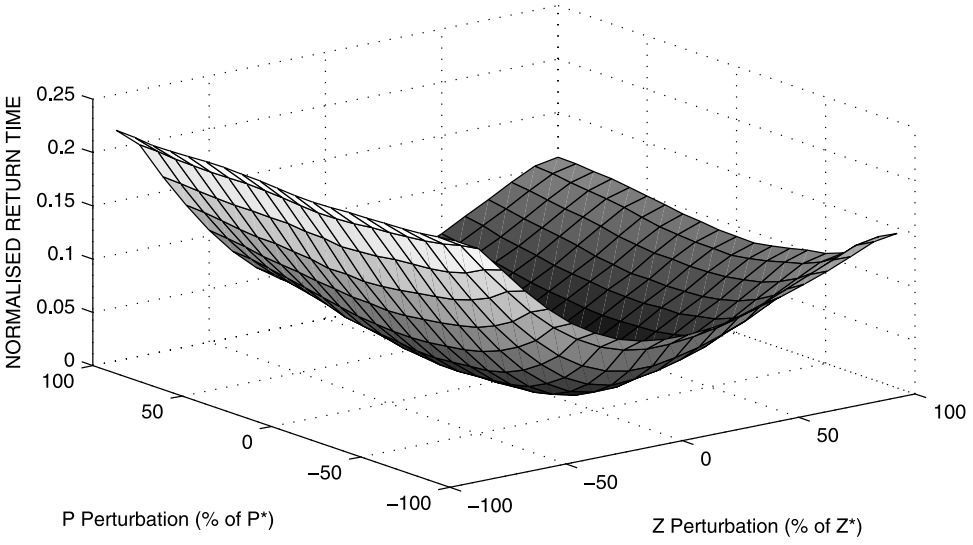

Figure 7. Normalized return time difference surface for the *NPZ-DMS* model with and without biogenic feedback. This surface is calculated by subtracting the return time surface of the *NPZ-DMS* model with feedback from the return time surface of the *NPZ-DMS* model with no feedback. This surface has been smoothed for clarity of presentation.

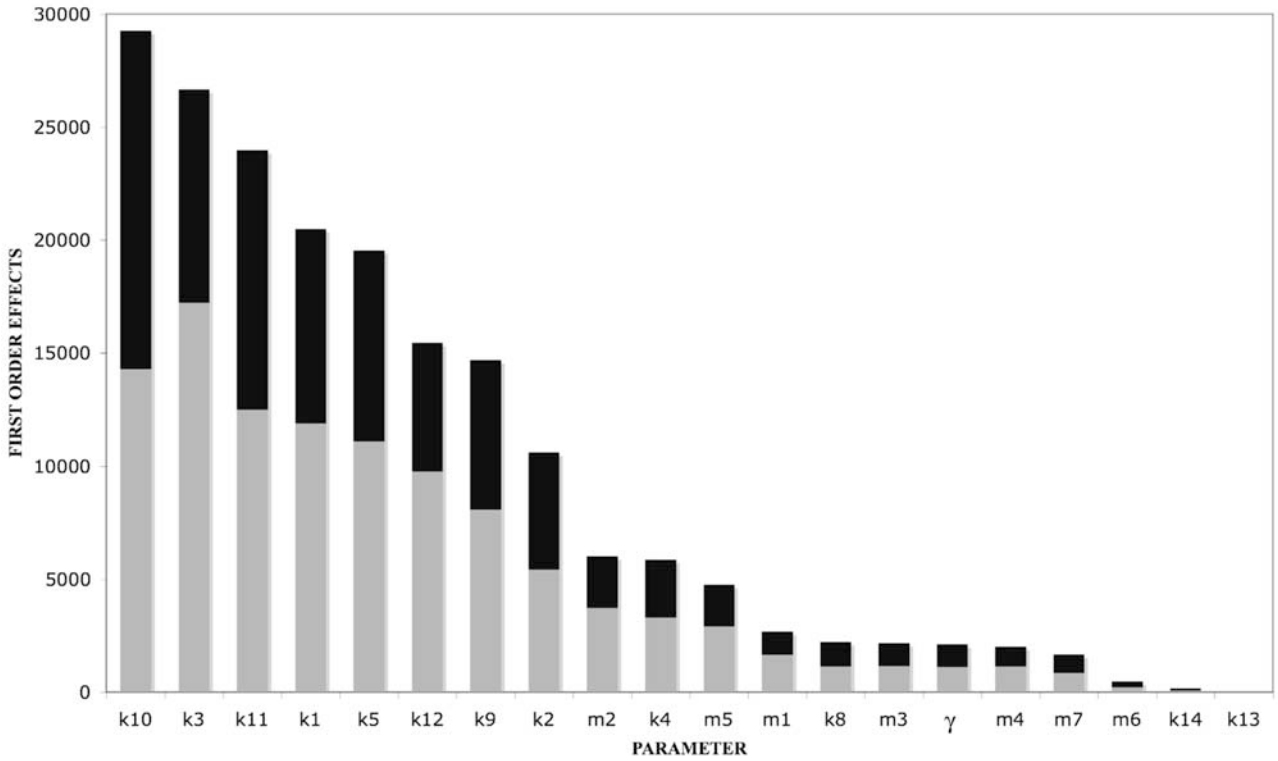

Figure 8. Sensitivity of feedback effect to first-order parameters identified by the New Morris Method. Light region of bar is sensitivity to each parameter alone; dark region is the influence of each parameter in association with all other parameters (i.e., indicates the existence of second- and higher-order interaction effects).

4.2. Return Time Surfaces

[52] The return time surface for the simple *NPZ* model without biogenic feedback on its environment is shown in Figure 5. This reveals that the model is more sensitive to perturbations in *Z* than to perturbations in *P*, in fact perturbations in *P* have almost no effect on the return time of the system if *Z* has suffered a large perturbation in either direction. This return time surface is characteristic of the *NPZ* model and is robust to substantial (but not all) parameter variations.

[53] The return time surface for the feedback model is shown in Figure 6. This return time surface is very similar to the surface for the *NPZ* model without biogenic feedback, the principal difference being that the feedback model returns to equilibrium more rapidly than the nonfeedback model.

[54] The surface representing the difference in return times to equilibrium for each of the models is shown in Figure 7. This surface clearly demonstrates that the inclusion of the biogenic feedback on its environment has endowed the *NPZ* model with increased resilience. The time the system requires to recover its equilibrium state after perturbations of any magnitude in any direction is substantially reduced by the inclusion of the feedback process. Similarly to the models' return time surfaces, the magnitude of the *P* perturbation does not have a substantial effect on the difference between the two return time surfaces. The magnitude by which the resilience is enhanced by the feedback process appears to be largely determined by the *Z* perturbation. For each *Z* perturbation, the *P* perturbations appear to have little influence on the return time of the system.

[55] This increased resilience is an interesting result as the feedback (R) is formulated so that at steady state $R = 1$ (its maximum possible value) and the resilience of the feedback model is identical to that of the nonfeedback model. Therefore including the feedback into the model cannot increase the resilience (as defined by equation (10)) of the model. The effect of the feedback when the *P* and *Z* populations are greater than their steady state values, the effect of the feedback is intuitive; it serves to reduce the irradiance the *P* receive and slows their growth rate, helping them to decline back to the steady state value. The effect on the system when the *P* and *Z* populations are smaller than their steady state values is not so intuitive; the *P* growth rate is again slowed, but it is not clear how this helps them to achieve their steady state values more rapidly.

4.3. Sensitivity Analysis

[56] All of the 48,400 comparisons of unlagged return time surfaces indicated that the biofeedback model returned to steady state more rapidly than the nonfeedback model, that is that the addition of the biogenic feedback always reduced the time taken for the system to recover from

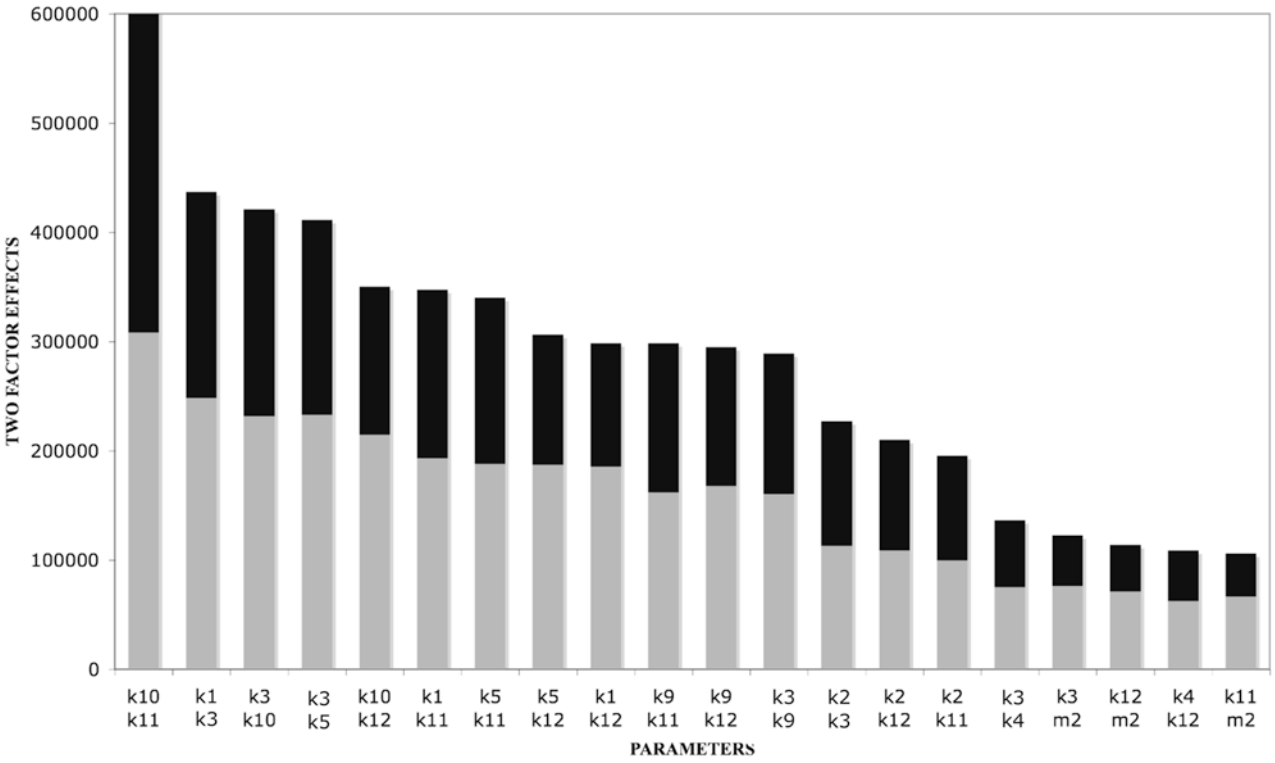

Figure 9. Sensitivity of feedback effect to second-order parameter interactions identified by the New Morris Method. Light region of bar is sensitivity to each parameter pair alone; dark region is the influence of each parameter pair in association with all other parameters (i.e., indicates the existence of third- and higher-order interaction effects).

perturbation. This result indicates that the stabilizing effect of adding the instantaneous feedback to the ecosystem model is robust to substantial parameter variations of both ecosystem and atmospheric processes.

[57] The sensitivity analysis indicated that the model return times after perturbation were sensitive to both biological parameters describing the ecosystem and physical parameters describing the atmospheric processes. Both the raw and normalized metrics used to measure the sensitivities (equations (43) and (44)) revealed almost the same sensitivities to the parameters. Only one of these, the raw sensitivities, are therefore presented, with Figure 8 describing the first-order effects and Figure 9 the second-order or two-parameter interaction effects. Two of the most influential parameters were k_{10} and k_{11}, describing the cloud droplet to CCN relationship (equation (20)), followed by k_3, the Z grazing rate, k_1, the P growth rate, and k_5, the Z mortality rate. It is apparent from equation (10) that these ecosystem rate parameters also have significant impacts on the model resilience.

[58] Combinations of these parameters were also important in the two-factor effects shown in Figure 9. While the two most influential parameter interactions, k_{10}, k_{11} and $k_{1,}$ k_3 are atmospheric and biological pairs respectively, the next most important pair $k_{3,}$ k_{10} and several other important pairs involving k_1, k_5, k_{11} and k_{12} reveal that interactions between the marine ecological processes and the atmospheric physical and chemical processes are important determinants of the magnitude of the feedback effect.

[59] The three important results from the sensitivity analysis are therefore that the consequences of the feedback for the ecosystem depend on both biological and atmospheric properties, that an instantaneous feedback always acts to stabilize the ecosystem dynamics, and that it is critically important to the determination of the actual magnitude of this feedback process that both the atmospheric and biological components of the process noted above are better quantified by field measurements.

4.4. Time Lag Analysis

[60] The time lag analysis reveals that the magnitude and direction of the feedback effect is dependent on the time lag between the ecosystem dynamics and the change in irradiance experienced by the phytoplankton as a result of the atmospheric feedback (Figure 10). The solid line in Figure 10 shows the effect of feedback time lags on the return time of the feedback model for the basic parameter set. This reveals that the initial stabilizing effect (by which is meant that the resilience the system is increased) of the feedback, where it reduces the return time of the model by about 6%, rapidly declines once a lag of two days is introduced into the feedback. The feedback has no effect on the resilience of the model if the feedback is lagged by three days, and for lags of three to six days, the feedback

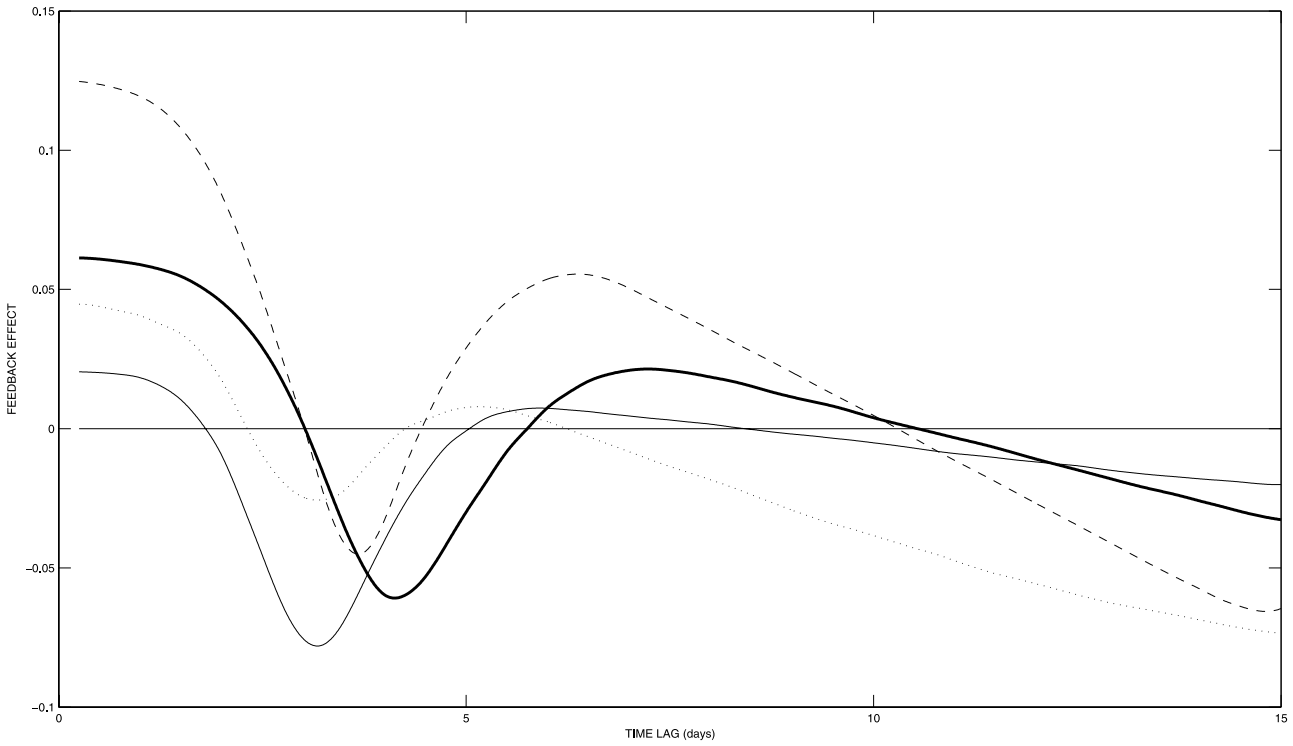

Figure 10. Effect of time lags on the feedback for the return time of the *NPZ-DMS* feedback model. The feedback effect is measured as the proportion by which sum of nonfeedback model's return time surface exceeds the sum of the feedback model's return time surface. The thick solid line is the feedback model with the default parameter set, the dotted line is with the maximum phytoplankton growth rate (k_1) doubled, the dashed line is with the zooplankton grazing rate (k_3) doubled, and the thin solid line is with the zooplankton mortality rate (k_5) doubled.

destabilizes (reduces the resilience of) the model, increasing the return time by up to about 6%.

[61] Time lags of six to ten days once again increase the resilience of the feedback model (by up to about 2%). This recovery of the stabilizing effect of the feedback, with a maximum in the second stabilizing region at a time lag of about seven days is especially interesting given that ocean in situ ecosystem-scale experiments that stimulated phytoplankton blooms measured a peak in DMS aqueous concentrations about a week after the bloom [*Turner et al.*, 1996]. Time lags greater than ten days again result in destabilization of the feedback model. It should be noted, however, that while the lagged feedback sometimes makes this model less resilient, causing it to take up to 10% longer to reach steady state than the nonfeedback model (Figure 10), it never reduces the resilience to zero (i.e., the system always returns to the steady state). For the realistic (i.e., based on measured values) parameter values used (Tables 1 and 2) both models are always stable; only the resilience, and hence the time taken to return to steady state after a perturbation, is affected by the feedback.

[62] The time lag analysis also reveals the influence that the properties of the biota in the ecosystem can have on the feedback process. The simulation with k_1 doubled (Figure 10, dotted line) reveals that the increased phytoplankton growth rate both greatly reduces the time lags for which the feedback model is initially more resilient (two days rather than three) and also reduces the magnitude of the stabilizing or destabilizing effects (a 4% reduction in return time). Similarly the recovery of the stabilizing effect occurs earlier (around four days), but lasts for only two days and produces only a 1% reduction in return time.

[63] The simulation with doubled zooplankton grazing (k_3) reveals quite the opposite effect (Figure 10, dashed line). In this case the increase in resilience for lags of up to three days is substantially increased with return times being up to 12.5% shorter than the nonfeedback model. The region of reduced resilience is smaller and the stabilizing effect is recovered much sooner at about 4 days. This variant also recovers resilience to a greater extent than the base parameter feedback model, with reductions in return time of up to 6%. The reduction in resilience that subsequently occurs is again very similar to the base parameter feedback model. The distinctive feature of the increased zooplankton grazing model is that its region of reduced resilience in Figure 10 is much smaller (in magnitude and duration) compared to both other parameter options.

[64] An increase in the rate of zooplankton mortality (k_5) also reduces the stabilizing effect of the feedback, reducing its initial increase in resilience to about 2%, but providing

the largest reduction in resilience of over 7.5% at about day three. This variant also reduces the duration of the initial stabilizing feedback to less than 2 days. The feedback again produces increased resilience after a time lag of 5 days, and remains so up to about 8 days, but only marginally (less than 1% reduction in return time). However, subtle effects that operate for long periods of time may still be influential.

[65] An interesting aspect of the response of the feedback effect to these parameter variations is that the feedback process provides the ecosystem with a mechanism to recover resilience if the attributes of the biota change to reduce it. Increases in the phytoplankton growth rate (k_1) and the zooplankton mortality rate (k_5) reduce the stabilizing effect of the feedback, but it is apparent from equation (10) that they simultaneously must increase the resilience of the ecosystem. Similarly, increases in the zooplankton grazing rate (k_3) reduce the resilience of the ecosystem, but increase the stabilizing effect of the feedback. Of these two processes, the ecosystem resilience is the principal determinant of the response to perturbation; the feedback system with increased phytoplankton growth rate has shorter return times than the system with increased zooplankton grazing, even though the latter provides a much greater stabilizing feedback effect. An interesting heuristic gained from this analysis is that the feedback process provides a ''resilience insurance policy'' in that changes in the properties of the ecosystem that tend to reduce its resilience are countered by an increase in resilience delivered by the feedback, and vice versa.

5. Discussion

[66] This research essentially generates a hypothesis that the DMS feedback process may serve to stabilize (that is, increase the resilience of) some ecosystems. The geographical extent to which this hypothesis may apply is as yet unclear, as the *NPZ-DMS* model is not able to reproduce chlorophyll and DMS dynamics over the whole of the global oceans. The stability attributes of the *NPZ* and *DMS* models suggest that the model will be best able to reproduce observed dynamics in regions of the oceans where the chlorophyll seasonal variation closely follows the physical forcings of irradiance, temperature and mixed layer depth, and the DMS concentration is closely coupled to the chlorophyll signal. This is generally the situation in high latitudes where the forcings are very strong and drive the plankton dynamics, but is not the case in many parts of the oceans. In the equatorial oceans, for example, chlorophyll is often out of phase with the physical forcings, and this model cannot reproduce the temporal chlorophyll dynamics in these regions. Similarly, the model cannot reproduce DMS dynamics if there is a substantial time lag between the chlorophyll maximum and the DMS maximum, for example the ''summer paradox'' observed at some mid- and low-latitude locations [*Simó and Pedrós-Alió*, 1999].

[67] These caveats constrain the spatial range where the model can competently reproduce measured data, but do not necessarily degrade the heuristic value of the model. Work in progress by the authors suggests that the dynamics of the *NPZ* model used in this analysis is a subset of a slightly more complicated *NPZ* model that can fit chlorophyll dynamics that are out of phase with their physical forcings. (The dynamics of this slightly more complicated model are such that at this stage it does not have the heuristic value of the model we have used.) Similarly, S. Vallina et al. (A dynamic model of oceanic sulfur (DMOS) applied to the Sargasso Sea: Simulating the dimethylsulfide (DMS) summer paradox, submitted to *Journal of Geophysical Research*, 2007) show that the DMS summer paradox may be explained by including an extra DMS source term, reflecting the exudation of DMS by phytoplankton under UV stress, that effectively loosens the coupling between the ecosystem and chemical models.

[68] Although there are no assumptions in the model that intrinsically limit its application to any part of the globe, the validation exercise suggests that inferences and hypotheses drawn from this exercise may only be directly relevant to high-latitude regions. Nevertheless, this research contributes a new dimension to the DMS hypothesis of *Charlson et al.* [1987] in particular, and to the field of Earth System Science in general. Our results show that an instantaneous biogenic feedback on the planktonic ecosystem model's irradiance environment can make the model more resilient to perturbation. The time that the system requires to return to its equilibrium state after any perturbation is therefore reduced by the addition of the instantaneous feedback.

[69] The stabilizing effect of the feedback is largest for perturbations that reduce the Z population. This is an interesting result, as recent work on model *NPZ* ecosystems [*Cropp and Norbury*, 2007] suggests that extinction processes in climate change scenarios will progress sequentially commencing with the extinction of Z. The presence of the feedback mechanism in the model therefore provides the system with an additional safeguard against extinction: the smaller the Z population gets, the stronger the feedback restoring the system to its equilibrium state becomes. This suggests the heuristic that the stability properties engendered by the feedback act most strongly in the manner required to both save the species and to maintain the ecosystem in its original form.

[70] The sensitivity analysis revealed two important properties of the instantaneous feedback effect: that it always serves to increase the resilience of the model, and that it is a function of both the biological and physical-chemical factors involved in the process. Two important parameters controlling the magnitude of the feedback effect are the slope (k_{10}) and intercept (k_{11}) values of the regression relating the number of cloud droplets in the atmosphere to the number of cloud condensing nuclei in the atmosphere. The second most influential parameter is the rate of zooplankton grazing on phytoplankton (k_3). This parameter was identified by *Cropp et al.* [2004] as the most important determinant of annual integrated DMS flux to the atmosphere.

[71] The time lag analysis revealed that the magnitude of the feedback effect, and whether it increases or reduces the resilience of the system, depends on the time lags associated with the feedback processes. This analysis revealed that the feedback could make the system more sensitive to perturbation if the effect of the feedback took several days to impact on the ecosystem. However, the most interesting and perhaps important result of the time lag analysis is that for

time lags of about 7–10 days the feedback effect again increases the resilience of the ecosystem; that is the feedback causes the ecosystem to return to its equilibrium state more rapidly than if the feedback was not present. The time lags that lead to this recovered stabilizing effect correspond with time lags observed in in situ ocean ecosystem experiments between phytoplankton blooms and subsequent maximum aqueous DMS concentrations [*Turner et al.*, 2004, 1996]. This analysis also identified an important modification to the results of the sensitivity analysis that also serves to further reflect the importance of k_1, k_3 and k_5 on the stabilizing effects of the feedback, and suggest that the timing and magnitude of the feedback effects will vary between ecosystems.

[72] The time-lagged feedback model we have used does not account for spatial factors, and the rapid advection rates in the atmosphere compared to the ocean suggest that only in periods of calm weather would the atmospheric effects generated by a phytoplankton bloom affect the originating population. However, as the atmospheric processes involved in the feedback may be rapid [*Hamilton and Lenton*, 1998], for some pathways perhaps as short as six hours [*Lin and Chameides*, 1993], couplings on local and regional scales may be close.

[73] The influence of the feedback on the ecosystem model's stability characteristics leads to the interesting hypothesis that the DMS feedback cycle may not be just an artifact of plankton biochemistry, but an intrinsic component of marine planktonic ecosystems. Such a hypothesis would suggest that marine phytoplankton gained a benefit from the production of DMSP as it initiated processes that stabilized the plankton ecosystem and consequently buffered the population from the effects of perturbations. Many authors, perhaps beginning with *Dunbar* [1960], have pointed to the susceptibility of populations to extinction due to stochastic events when at the nadir of extended "boom and bust" cycles that many low-resilience systems experience after perturbation.

[74] Such a hypothesis would require the invocation of group selection, a concept extensively attacked in the 1970s [see, e.g., *Dawkins*, 1976]. While it is not the intent of this research to debate the merits of group selection, we note that group selection is attracting new interest in western evolutionary debate [*Borello*, 2005] and that ecosystem evolution is an accepted paradigm in Russian science [*Lekiavichius*, 2003]. As noted by *Loreau et al.* [2004] "Species traits and their evolution are ultimately constrained by ecosystem processes, just as ecosystem properties are constrained by the ecological and evolutionary history of interacting species."

[75] Our results clearly show that the influence of the feedback is dependent on the time lags in the ocean and atmospheric processes, and on the characteristics of the ecosystem. Our theoretical analysis suggests that clarification of the timescales of the feedback processes, and better knowledge of all the parameters in the model, would be a very useful contribution to the whole DMS hypothesis.

6. Conclusion

[76] This research has modeled a process whereby production of a precursor compound by individual phytoplankton, coupled with subsequent biological processing by coconstituents of a plankton ecosystem, results in a product that modifies the properties of the atmosphere. The changes in albedo we have modeled subsequently influence the irradiance experienced by the phytoplankton that initiated the process. Our results demonstrate that this change in environment modifies the population dynamics of the phytoplankton and may make the ecosystem to which they belong more resilient to perturbation. Our results also suggest that the magnitude and timing of the feedback effects are highly dependent on the characteristics the ecosystems and the atmospheric processes involved. Although the feedback effect can reduce the resilience of the ecosystem when time lags are introduced, the feedback increases the resilience of the system at time lags similar to those observed in real ocean plankton ecosystems.

[77] The coherence of these theoretical and observed relationships then raises the question of whether the phytoplankton-DMS-cloud relationship reflects a fortuitous artifact of phytoplankton metabolism or an evolved property that improves phytoplankton fitness by stabilizing the dynamics of their ecosystem. Because the benefits derived by an individual phytoplankton from producing DMSP are accrued by the group, and perhaps even the ecosystem as a whole, the option that phytoplankton have evolved the ability to influence the properties of the atmosphere invokes group-level selection. *Hamilton and Lenton* [1998] have argued just such a case for these systems, although in support of a different hypothesis. The stabilizing effects observed in this study, although subtle, would act over long timescales and may therefore have profound implications for the characteristics of the ecosystems that generate them.

[78] Our research indicates a pressing need for clarification of the timescales of the atmospheric processes involved in the DMS feedback. Although the feedback effects we have documented appear robust to substantial parameter variations the implications of the feedback process for marine plankton ecosystems may not be fully assessed, nor our hypothesis refined, until these details are elucidated. If the time lags observed in real systems do indeed correspond with the time lags that stabilize our model ecosystem, then such further research may yield rich results relating to fundamental properties of living systems.

[79] **Acknowledgments.** This research was funded by an Australian Research Council Discovery Grant to Roger Cropp. The authors wish to acknowledge the various contributions of Albert Gabric, Kees Hulsman, Rachel King, and Mark Ponniah to this work. The authors would also like to thank the SeaWiFS Project (Code 970.2) and the Distributed Active Archive Centre (Code 902) at the Goddard Space Flight Centre, Greenbelt, Maryland, for the production and distribution, respectively, of the SeaWiFS data. These activities are sponsored by NASA's Mission to Planet Earth Program (http://seawifs.gsfc.nasa.gov). The Quikscat/SeaWinds and Advanced Very High Resolution Radiometer data was obtained from the NASA Physical Oceanography Distributed Active Archive Centre at the Jet Propulsion Laboratory, California Institute of Technology (http://podaac.jpl.nasa.gov). The World Ocean Atlas 1994 data were provided by the NOAA-CIRES Climate Diagnostics Center, Boulder, Colorado (http://www.cdc.noaa.gov/). Finally, the authors would like to thank two very thorough but anonymous reviewers for their substantial contributions to this manuscript.

References

Andreae, M. O., W. Elbert, and S. J. de Mora (1995), Biogenic sulphur emissions and aerosols over the tropical South Atlantic: 3. Atmospheric dimethylsulphide, aerosols and cloud condensation nuclei, *J. Geophys. Res.*, *100*, 11,335–11,356.

Ayers, G. P., and R. W. Gillett (2000), DMS and its oxidation products in the remote marine atmosphere: Implications for climate and atmospheric chemistry, *J. Sea Res.*, *43*, 275–286.

Borello, M. E. (2005), The rise, fall and resurrection of group selection, *Endeavour*, *29*, 43–47.

Campolongo, F., and R. Braddock (1999), The use of graph theory in the sensitivity analysis of the model output: A second order screening method, *Reliab. Eng. Syst. Safety*, *64*, 1–12.

Charlson, R. J., J. E. Lovelock, M. O. Andreae, and S. G. Warren (1987), Oceanic phytoplankton, atmospheric sulphur, cloud albedo and climate, *Nature*, *326*, 655–661.

Chuang, C. C., and J. E. Penner (1995), Effects of anthropogenic sulphate on cloud drop nucleation and optical properties, *Tellus, Ser. B*, *47*, 566–577.

Cropp, R. A., and R. D. Braddock (2002), The New Morris Method: An efficient second-order screening method, *Reliab. Eng. Syst. Safety*, *78*, 77–83.

Cropp, R. A., and A. J. Gabric (2002), Ecosystem adaptation: Do ecosystems maximise resilience?, *Ecology*, *83*, 2019–2026.

Cropp, R. A., and J. Norbury (2007), Investigations into a plankton population model: Mortality and its importance in climate change scenarios, *Ecol. Modell.*, *201*, 97–117.

Cropp, R. A., J. Norbury, A. Gabric, and R. Braddock (2004), Modeling dimethylsulphide production in the upper ocean, *Global Biogeochem. Cycles*, *18*, GB3005, doi:10.1029/2003GB002126.

Dawkins, R. (1976), *The Selfish Gene*, Oxford Univ. Press, Oxford, U. K.

DeAngelis, D. L. (1980), Energy flow, nutrient cycling and ecosystem resilience, *Ecology*, *61*, 764–771.

Dunbar, M. J. (1960), The evolution of stability in marine environments: Natural selection at the level of the ecosystem, *Am. Nat.*, *94*, 129–136.

Eppley, R. W. (1972), Temperature and phytoplankton growth in the sea, *Fish. Bull.*, *70*, 1063–1085.

Franks, P. J. S. (2002), NPZ models of plankton dynamics: Their construction, coupling to physics, and application, *J. Oceanogr.*, *58*, 379–387.

Gabric, A. J., N. Murray, L. Stone, and M. Kohl (1993), Modeling the production of dimethylsulfide during a phytoplankton bloom, *J. Geophys. Res.*, *98*, 22,805–22,816.

Gabric, A. J., P. A. Matrai, and M. Vernet (1999), Modelling the production and cycling of dimethylsulphide during the vernal bloom in the Barents Sea, *Tellus, Ser. B*, *51*, 919–937.

Goldman, J. C., and E. L. Carter (1974), A kinetic approach to the effect of temperature on algal growth, *Limnol. Oceanogr.*, *19*, 756–766.

Gondwe, M. (2004), Quantifying the role of marine phytoplankton in the present day climate system, 129 pp., Ph.D. thesis, Fac. of Math. and Nat. Sci., Univ. of Groningen, Groningen, Netherlands.

Gultepe, I., and G. A. Isaac (1996), The relationship between cloud droplet and aerosol number concentrations for climate models, *Int. J. Climatol.*, *16*, 941–946.

Hamilton, W. D., and T. M. Lenton (1998), Spora and Gaia: How microbes fly with their clouds, *Ethol. Ecol. Evol.*, *10*, 1–16.

Han, Q., W. B. Rossow, J. Chou, and R. M. Welch (1998), Global survey of the relationships of cloud albedo and liquid water path with droplet size using ISCCP, *J. Clim.*, *11*, 1516–1528.

Hegg, D. A. (1994), Cloud condensation nucleus-sulfate mass relationship and cloud albedo, *J. Geophys. Res.*, *99*, 25,903–25,907.

Holland, J. H. (1975), *Adaptation in Natural and Artificial Systems*, 211 pp., Univ. of Mich. Press, Ann Arbor.

Johnson, L. (1990), The thermodynamics of ecosystems, in *The Handbook of Environmental Chemistry,* vol. 1E, *The Natural Environment and the Biogeochemical Cycles*, edited by O. Hutzinger, pp. 1–47, Springer, Berlin.

Kettle, A. J., et al. (1999), A global database of sea surface dimethylsulfide (DMS) measurements and a procedure to predict sea surface DMS as a function of latitude, longitude and month, *Global Biogeochem. Cycles*, *13*, 399–444.

Kiene, R. P., L. J. Linn, and J. A. Bruton (2000), New and important roles for DMSP in marine microbial communities, *J. Sea Res.*, *43*, 209–224.

Lawrence, M. G. (1993), An empirical analysis of the strength of the phytoplankton-dimethylsulfide-cloud-climate feedback cycle, *J. Geophys. Res.*, *98*, 20,663–20,673.

Laws, E. A. (2003), Partitioning of microbial biomass in pelagic aquatic communities: maximum resiliency as a food web organizing construct, *Aquat. Microb. Ecol.*, *32*, 1–10.

Lekiavichius, E. (2003), Ecosystem evolution: Main stages and potential mechanisms, *Zh. Obshch. Biol.*, *64*, 371–388.

Lin, X., and W. L. Chameides (1993), CCN formation from DMS oxidation without SO2 acting as an intermediate, *Geophys. Res. Lett.*, *20*, 579–582.

Liss, P. S., and L. Merlivat (1986), Air-sea gas exchange rates: Introduction and synthesis, in *The Role of Air-Sea Exchange in Geochemical Cycling*, edited by P. Buat-Menard, pp. 113-127, D. Reidel, Norwell, Mass.

Loreau, M., C. de Mazancourt, and R. D. Holt (2004), Ecosystem evolution and conservation, in *Evolutionary Conservation Biology*, edited by R. Ferriere et al., pp. 327–343, Cambridge Univ. Press, Cambridge, U. K.

Mitchell, M. (1997), *An Introduction to Genetic Algorithms*, 208 pp., MIT Press, Cambridge, Mass.

Moloney, C. L., M. O. Bergh, J. G. Field, and R. C. Newell (1986), The effect of sedimentation and microbial nitrogen regeneration in a plankton community: A simulation investigation, *J. Plankton Res.*, *8*, 427–445.

Neubert, M. G., and H. Caswell (1997), Alternatives to resilience for measuring the responses of ecological systems to perturbations, *Ecology*, *78*, 653–665.

Nightingale, P. D., G. Malin, C. S. Law, A. J. Watson, P. S. Liss, M. I. Liddicoat, and J. Boutin (2000), In situ evaluation of air-sea gas exchange parameterizations using novel conservative and volatile tracers, *Global Biogeochem. Cycles*, *14*, 373–387.

Pandis, S. N., L. M. Russell, and J. H. Seinfeld (1994), The relationship between DMS flux and CCN concentration in remote marine regions, *J. Geophys. Res.*, *99*, 16,945–16,957.

Saltzman, E. S., D. B. King, K. Holmen, and C. Leck (1993), Experimental determination of the diffusion coefficient of dimethylsulfide in water, *J. Geophys. Res.*, *98*, 16,481–16,486.

Saxena, V. K., and S. Menon (1999), Sulfate-induced cooling in the southeastern U.S.: An observational assessment, *Geophys. Res. Lett.*, *26*, 2489–2492.

Schwartz, S. E., and A. Slingo (1996), Enhanced shortwave cloud radiative forcing due to anthropogenic aerosols, in *Clouds, Chemistry and Climate*, edited by P. J. Crutzen and V. Ramanathan, pp. 191–235, Springer, Berlin.

Simó, R. (2001), Production of atmospheric sulfur by oceanic plankton: Biogeochemical, ecological and evolutionary links, *Trends Ecol. Evol.*, *16*, 287–294.

Simó, R., and J. Dachs (2002), Global ocean emission of dimethylsulfide predicted from biogeophysical data, *Global Biogeochem. Cycles*, *16*(4), 1018, doi:10.1029/2001GB001829.

Simó, R., and C. Pedrós-Alió (1999), Role of vertical mixing in controlling the oceanic production of dimethyl sulphide, *Nature*, *402*, 396–399.

Sunda, W., D. J. Kieber, R. P. Kiene, and S. Huntsman (2002), An antioxidant function for DMSP and DMS in marine algae, *Nature*, *418*, 317–320.

Turner, S. M., P. D. Nightingale, L. J. Spokes, M. I. Liddicoat, and P. S. Liss (1996), Increased dimethylsulphide concentrations in sea water from in situ iron enrichment, *Nature*, *383*, 513–517.

Turner, S. M., M. Harvey, C. S. Law, P. D. Nightingale, and P. S. Liss (2004), Iron-induced changes in oceanic sulfur biogeochemistry, *Geophys. Res. Lett.*, *31*, L14307, doi:10.1029/2004GL020296.

Walsh, J., D. A. Dieterle, and J. Lenes (2001), A numerical analysis of carbon dynamics of the Southern Ocean phytoplankton community: The roles of light and grazing in effecting both sequestration of atmospheric CO_2 and food availability to larval krill, *Deep Sea Res., Part I*, *48*, 1–48.

Wolfe, G. V., M. Steinke, and G. O. Kirst (1997), Grazing-activated chemical defence in a unicellular marine alga, *Nature*, *387*, 894–897.

Zonneveld, C. (1998), Photoinhibition as affected by photoacclimation in phytoplankton: A model approach, *J. Theor. Biol.*, *193*, 115–123.

R. Braddock and R. Cropp, Centre for Environmental Systems Research, Faculty of Environmental Sciences, Griffith University, Kessels Road, Nathan, Qld 4111, Australia. (r.braddock@griffith.edu.au; r.cropp@griffith.edu.au)

J. Norbury, Mathematical Institute, University of Oxford, 24-29 St Giles, Oxford OX3 9DU, UK. (john.norbury@lincoln.oxford.ac.uk)